

# Keto–enol tautomerism of two structurally related Schiff bases: Direct and indirect way of creation of the excited keto tautomer

P. Fita <sup>a,\*</sup>, E. Luzina <sup>b</sup>, T. Dziembowska <sup>c</sup>, D. Kopeć <sup>a</sup>, P. Piątkowski <sup>d</sup>,  
Cz. Radzewicz <sup>a,b</sup>, A. Grabowska <sup>b</sup>

<sup>a</sup> *Institute of Experimental Physics, Warsaw University, ul. Hoża 69, 00-681 Warsaw, Poland*

<sup>b</sup> *Institute of Physical Chemistry, Polish Academy of Sciences and Laser Center, Kasprzaka 44/52, 01-224 Warsaw, Poland*

<sup>c</sup> *Institute of Fundamental Chemistry, Technical University of Szczecin, Aleja Piastów 42, 71-065 Szczecin, Poland*

<sup>d</sup> *Faculty of Chemistry, Warsaw University, Żwirki i Wigury 101, 02-089 Warsaw, Poland*

Received 18 July 2005; in final form 16 September 2005

Available online 12 October 2005

## Abstract

Femtosecond time-resolved absorption spectra of two structurally related, internally H-bonded Schiff bases are reported. The 2-hydroxynaphthylidene-1'-naphthylamine (HNAN) stable as an enol tautomer undergoes an ultrafast excited state intramolecular proton transfer, while the 2-hydroxynaphthylidene-(8'-aminoquinoline) (HNAQ), stable as a keto structure, reveals unusual relaxation routes after electronic excitation. In particular, the rise of the bleaching band with the characteristic time of  $\sim 700$  fs was found and attributed to a gradual population of the  $S_1$  fluorescent state from a 'hot' excited state. The results accompanied by TDDFT calculations are used to construct the diagram of relaxation routes of an excited HNAQ molecule.

© 2005 Elsevier B.V. All rights reserved.

## 1. Introduction

Some aromatic Schiff bases have been known for many decades as photochromic compounds [1]. This kind of photochromism represented, e.g., by salicylidene aniline (the best studied system of this class) is connected with the excited state intramolecular proton transfer (ESIPT) reaction [2]. Photochromism and ESIPT reactivity make this group of compounds very attractive from the point of view of several applications [3–5], as well as of purely academic studies of one of the fastest processes occurring in molecular systems [6]. On the other hand, the excited state proton transfer reactions, especially those 'prepared' by internal hydrogen bonds, are regarded as model processes particularly suitable and challenging for ultrafast laser techniques.

In this study, we report on two Schiff bases shown in Fig. 1. The first one – 2-hydroxynaphthylidene-1'-naphthylamine

(HNAN) – is stable in the ground state as an enol tautomer (in inert solvents), and the second one – 2-hydroxynaphthylidene-(8'-aminoquinoline) (HNAQ) – as a keto structure. These two compounds are examples of hydroxy derivatives of heteroaromatic molecules which typically undergo the ESIPT reaction from enol to keto tautomer. The excited keto structure returns to the ground state emitting fluorescence and/or undergoing the *cis–trans* isomerization, which gives birth to the photochromic transient, and eventually restores the initial enol structure closing up the so called proton transfer (PT) cycle.

The ultimate goal of our work is to follow the PT cycle in order to explore two routes: one – involving the ESIPT reaction from enol to keto tautomer, represented by HNAN molecule, and the other – 'reversed' – in which the molecule in the keto form is excited and relaxes back to the ground state via some traps, such as a photochromic isomer or a triplet state, represented by HNAQ. In this Letter, we report on the results for HNAN and HNAQ obtained with several stationary spectral techniques, as well as femtosecond

\* Corresponding author. Fax: +48 22 625 64 06.

E-mail address: [fita@fuw.edu.pl](mailto:fita@fuw.edu.pl) (P. Fita).

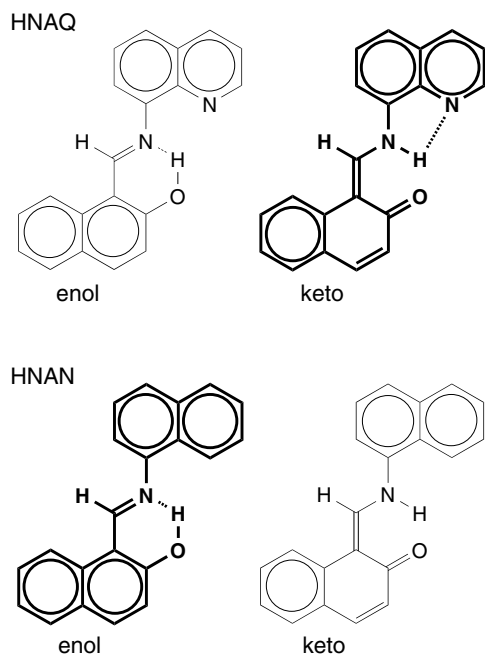


Fig. 1. Formulae of enol and keto-tautomers of HNAQ and HNAN. Tautomers stable in the ground state are printed in bold.

time-resolved absorption spectra. We also analyze the ultra-fast kinetics of a HNAQ molecule; the full discussion and comparison between the two molecules will be the subject of a forthcoming Letter.

The literature data on both systems are rather scarce. The NMR spectra of HNAN and HNAQ in the solid state [7] and  $\text{CDCl}_3$  solution [8] have been measured just recently. According to study [7], involving the  $^{13}\text{C}$  and  $^{15}\text{N}$  CPMAS methods, as well as deuterium isotope effects on  $^{15}\text{N}$  chemical shifts, HNAQ molecule exists as a pure keto tautomer, while HNAN in the solid state is present as keto tautomer with some fraction of the enol form. The latter is almost in agreement with the X-rays data [9] stating full planarity of this molecule and its keto tautomeric structure. The stationary absorption spectra of both molecules studied as a function of polarity of the solvent were reported by Abbas et al. [10]. The main conclusion of this study was that HNAN molecule is stable in the ground state at room temperature as an enol tautomer, while HNAQ is present as a keto form even in solvents normally favouring enol structures of similar systems. According to Abbas and co-workers, the reason for this unusual behavior is the bifurcated H-bond whose proton donor, NH group, interacts with both the quinoline nitrogen atom and carbonyl oxygen. The most recent paper [11] reporting on the spectra of several Schiff bases, derivatives of salicylidene aniline, shows again the absorption of HNAN, as a function of polarity of the solvent. The authors reproduced the results of [10] performed at room temperature, clearly overlooking this work. They showed that upon lowering the temperature to 77 K a fairly strong fluorescence is observed, indicating that the enol–keto equilibrium of HNAN is totally

shifted towards the keto tautomer. Surprisingly, they did not observe the same fluorescence at room temperature even though, as we have shown below, it can be registered with a standard spectrofluorometer.

## 2. Experimental

HNAQ and HNAN were synthesized by a standard method of condensation of 2-hydroxynaphthaldehyde with corresponding amines in refluxing ethanol. The purity was checked by NMR spectra. Melting points are: 222–223 and 182–183 °C for HNAQ and HNAN, respectively.

Stationary absorption spectra were measured with Shimadzu UV 3100 spectrometer. Steady-state fluorescence and lifetimes of fluorescent states were measured with FS and FL 900 CDT spectrofluorometer, Edinburgh Instruments. Transient absorption measurements were carried out in a typical setup modelled on the original one presented in [12]. All experiments with HNAQ were performed in tetrahydrofuran (THF) which was carefully purified and distilled before each experiment. Methylcyclohexane (MCHX) ‘for HPLC chromatography’ from Sigma–Aldrich was used, as supplied, as a solvent for HNAN.

Quantum chemical calculations were performed with the aid of the GAUSSIAN 98 program package [13] with the 6-31G(d,p) basis set. The ground state geometry was optimized by DFT/B3LYP method; transition energies were calculated with TDDFT [14] method.

## 3. Results

### 3.1. Stationary absorption and fluorescence

The stationary absorption and fluorescence spectra are shown in the lower panels of Fig. 2. For the HNAQ molecule the fluorescence excitation spectrum is also included. The spectra clearly show the difference between HNAQ and HNAN; for the first molecule the fluorescence band and the lowest absorption band reveal the so-called ‘mirror image symmetry’, while for HNAN the fluorescence band is shifted to the red by about  $7000\text{ cm}^{-1}$  with respect to the absorption maximum of the enol form. This is a typical behavior of a molecule undergoing a reaction in the excited state, thus the observed fluorescence is attributed to the keto tautomer.

The ‘mirror image’ relationship between absorption and fluorescence spectra usually implies the identity of the absorbing and fluorescent species. However, the case of HNAQ appears to be more complicated: the radiative lifetime calculated from the integrated absorption band with application of the classical Strickler–Berg formula [15] is equal to about 9 ns. The decay of the fluorescence measured at 536 and 640 nm is biexponential, with the shorter component being beyond the temporal resolution of the instrument, and the longer one close to 12 ns. A good agreement between the measured and calculated decay times implies that the fluorescence quantum yield should

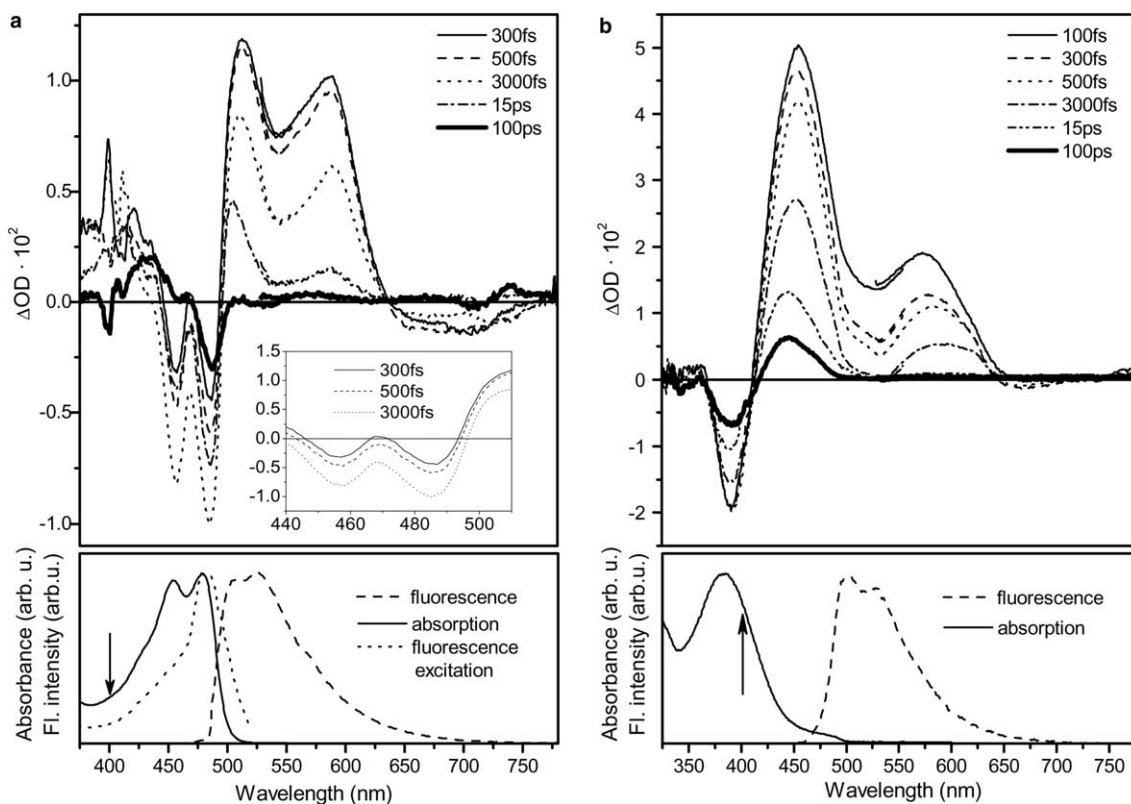


Fig. 2. Transient absorption spectra of: (a) HNAQ and (b) HNAN. The inset shows the raise of the bleaching band. Stationary absorption, fluorescence, and fluorescence excitation (for HNAQ only) spectra are shown at the bottom. Excitation wavelength is marked with an arrow.

be of the order of unity. This is in contrast to the experimental value of the fluorescence quantum yield, which is  $(3.5 \pm 0.5) \times 10^{-3}$  as measured with quinine sulfate standard [16]. Moreover, the excitation spectrum of the stationary fluorescence differs from the absorption spectrum, as can be seen at the bottom of Fig. 2a. These observations lead to a conclusion, that HNAQ molecules in THF solution exist in the ground state as a mixture of two conformers of very similar spectral properties. A detailed discussion of this topic is presented below.

### 3.2. Time resolved absorption spectra

The upper panels of Fig. 2 show the time resolved spectra of both molecules. Three spectral regions common to both systems can be distinguished: the bleaching band that reflects the stationary absorption spectrum, the excited state absorption (ESA) band in the middle of the observed range, and the weak stimulated emission band located at the longest wavelengths.

Transient absorption signals of HNAN molecule rise instantaneously (within the time resolution of our system – 100–300 fs depending on the wavelength) at all wavelengths. In contrast, the bleaching band of HNAQ displays a finite risetime (see inset in Fig. 2a): it reaches its maximum about 3 ps after the excitation. Further analysis focuses on this molecule, while HNAN is regarded as a model structure for the inaccessible enol tautomer of

HNAQ. The close similarity of the structures of the ‘twin’ molecules makes this modelling reasonable.

Most signals disappear at the end of the available time window – 120 ps. The only remaining (long living ones) are the bleaching band partially hidden under the absorption band located around 430 nm (thick solid line in Fig. 2a).

The kinetics of transient signals at selected wavelengths are shown in Fig. 3. As the signal observed at the longest wavelengths – the stimulated emission band – was very weak, it was necessary to average it over a wide spectral range (675–725 nm) around its maximum in order to obtain its kinetics with an acceptable signal to noise ratio. Since, in this wavelength range, the emission seems to be disturbed only by a long-living (constant on the timescale of our experiment) ESA band, it was possible to determine its lifetime  $t_1 = (4.25 \pm 0.30)$  ps (see Table 1). This value cannot be directly verified by measurements of the fluorescence lifetime with a nanosecond spectrometer, nevertheless it was used in the fitting procedure of the nanosecond biexponential fluorescence decay as follows: one decay time was fixed at a value of 4.25 ps while the other was a parameter of the fit. As a result the slow component of the decay was obtained as  $(11.9 \pm 0.2)$  ns. Its amplitude is lower than the amplitude of the fast component by a factor of the order of  $10^3$ . This is the reason, why we do not observe long-living emission in the transient absorption spectrum.

The kinetics at shorter wavelengths are clearly not monoexponential which is a consequence of the fact that

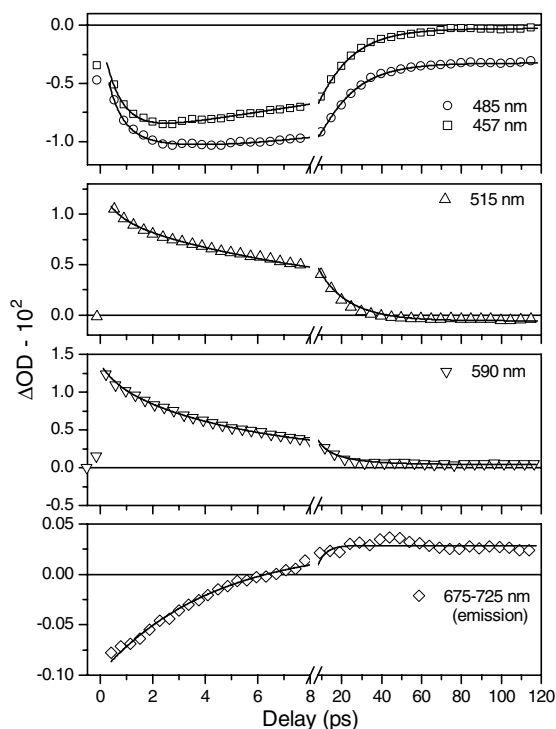


Fig. 3. Kinetics of transient absorption signals of HNAQ for selected wavelengths.

all transient bands overlap. It is reasonable to assume that one of the ESA bands comes from the same state as the stimulated emission, thus, when fitting these kinetics with biexponential curves, the first of the decay times was fixed at 4.25 ps. Then the second component ( $t_2$  in Table 1) was determined to be around 16 ps for the rest of the investigated wavelengths. Two ESA bands peaking around 515 and 590 nm differ by the contribution of these two components (the corresponding relative amplitudes are given in parentheses in Table 1).

In order to fit the kinetics in the range of the bleaching band (457 and 485 nm) it is necessary to take into account the finite risetime of this band ( $t_3$  in Table 1) which is around 0.7 ps.

At all wavelengths a component which is constant in the time range of the femtosecond experiment (120 ps) was found (its relative amplitudes are given in the last row in Table 1).

#### 4. Discussion

The first thing to be explained is the finite time at which the bleaching band reaches its maximum (inset in Fig. 2a) as it is not a common feature. One must remember that the bleaching signal observed in transient spectra at wavelengths corresponding to stationary absorption spectra originates predominantly due to the transition from the ground to electronically excited states and, as such, is proportional to the sum of two components. The first one is the number of molecules removed from the ground state due to optical excitation. The second component is the number of molecules occupying the upper level of the electronic transition responsible for stationary absorption. Frequently, this term is neglected or assumed to be equal to the first term. The first approach is justified, when – due to an ultrafast reaction in the excited state – optically excited molecules do not populate the upper level of the transition. The equality of both terms can be safely assumed when the upper level is populated directly by the pump pulse and relaxes back to the ground state. In both cases the kinetics of the bleaching signal reflects only the time-dependence of the population of the ground state.

Yet, the upper level of the transition responsible for the stationary absorption may be populated by relaxation from a higher lying state to which the molecule is excited by the pump pulse. In such a case the two terms defined above have different temporal behavior – the one which describes the number of molecules in the upper state raises with finite rate while the depopulation of the ground state is instantaneous. As a result, the kinetics of the bleaching signal consists of two components: a slower one reflecting the relaxation process in the excited state and the other raising instantaneously. In our case, HNAQ molecules are excited with a large excess of energy ( $4400 \text{ cm}^{-1}$ ) which well justifies the above mechanism.

More generally, the transient absorption at a given wavelength is the sum of the contributions from all excited states (e.g., as shown in Fig. 4,  $S_1$ ,  $S_2$ , the triplet states, and the excited rare conformer). They decay, however, independently, with lifetimes much longer than the risetime of the bleaching bands. On the other hand, their risetimes which can be observed at other wavelengths are much shorter

Table 1  
Numeric values of decay times for HNAQ for selected wavelengths

	675–725 nm	590 nm	515 nm	485 nm	457 nm
$t_1$ (ps)	$4.25 \pm 0.30$ ( $-0.81 \pm 0.04$ )	4.25 ( $0.75 \pm 0.03$ )	4.25 ( $0.44 \pm 0.03$ )	4.25 ( $0.19 \pm 0.05$ )	4.25 ( $0.26 \pm 0.07$ )
$t_2$ (ps)		$15 \pm 2$ ( $0.22 \pm 0.02$ )	$17 \pm 2$ ( $0.52 \pm 0.03$ )	$17 \pm 1$ ( $-0.46 \pm 0.03$ )	$15.3 \pm 0.5$ ( $-0.62 \pm 0.04$ )
$t_3$ (ps)				$0.83 \pm 0.16$ ( $0.22 \pm 0.02$ )	$0.60 \pm 0.06$ ( $0.11 \pm 0.01$ )
Constant	( $0.19 \pm 0.01$ )	( $0.036 \pm 0.003$ )	( $-0.042 \pm 0.003$ )	( $-0.13 \pm 0.01$ )	( $-0.01 \pm 0.01$ )

Relative amplitudes are given in parentheses. Value for  $t_1 = 4.25$  ps was determined from the kinetics of the stimulated emission band and set as fixed when fitting kinetics for other wavelengths. The last row shows the contribution of the constant component.

than the considered time range. Therefore, the transient signals originating from those levels form an approximately time-independent background and do not qualitatively change the described effect.

As discussed above, two structural modifications are present in the ground state of HNAQ. The main component dominates and the ‘rare’ one contributes to less than 1% of the total population. Moreover, because of the similarity of their absorption spectra they should have similar electronic structures. Most probably they are two conformers whose proposed structures are shown in the lower part of Fig. 4. The rare one emits the long living fluorescence with low apparent quantum yield, because the main component absorbs almost all light. In contrast, the main conformer emits the fluorescence with a very short lifetime. The fates of the rare conformer are not discussed here, since they are irrelevant from the point of view of fast events and we concentrate on the possible routes of relaxation of the main conformer shown on the left side of Fig. 4.

According to the results of TDDFT calculations, the lowest singlet ( $n,\pi^*$ ) state is situated almost exactly at the excitation energy ( $25000\text{ cm}^{-1}$ ) and the fluorescent  $S_1(\pi,\pi^*)$

level has in its proximity two triplet states,  $T_4(n,\pi^*)$  and  $T_3(\pi,\pi^*)$ . Two lowest triplet states,  $T_2(\pi,\pi^*)$  and  $T_1(\pi,\pi^*)$  are situated at about  $20000\text{ cm}^{-1}$  and  $15000\text{ cm}^{-1}$  as shown in Fig. 4.

The excitation of HNAQ by a laser pulse provides a high energy excess. The process of relaxation lasting about 0.7 ps involves partial population of the  $S_2(n,\pi^*)$  state and creation of a long living trap. The 16 ps lifetime which we attribute to the  $S_2(n,\pi^*)$  state cannot be recovered in the decay of the  $S_1$  fluorescence. Thus we suppose that the  $S_2$  state is populated in a one-way process ( $S_1^{**} \rightarrow S_2$ ) and relaxes independently from the  $S_1$  state. The rest of ‘hot’ molecules relaxes to the  $S_1(\pi,\pi^*)$  fluorescent state. This relaxation is observed as a rise in the bleaching. The fluorescent  $S_1$  state is very effectively depopulated via the cascade of triplet states, two of them,  $T_3(\pi,\pi^*)$  and  $T_4(n,\pi^*)$  being the nearby states. This is the reason for a dramatic shortening of its lifetime seen as the fast decay of the stimulated emission in the femtosecond experiment.

The long living trap, seen as the absorption band centred around 430 nm, most probably may be attributed to the  $T_n \leftarrow T_1$  absorption from the lowest  ${}^3(\pi,\pi^*)$  triplet state. The existence of this long living trap is also reflected

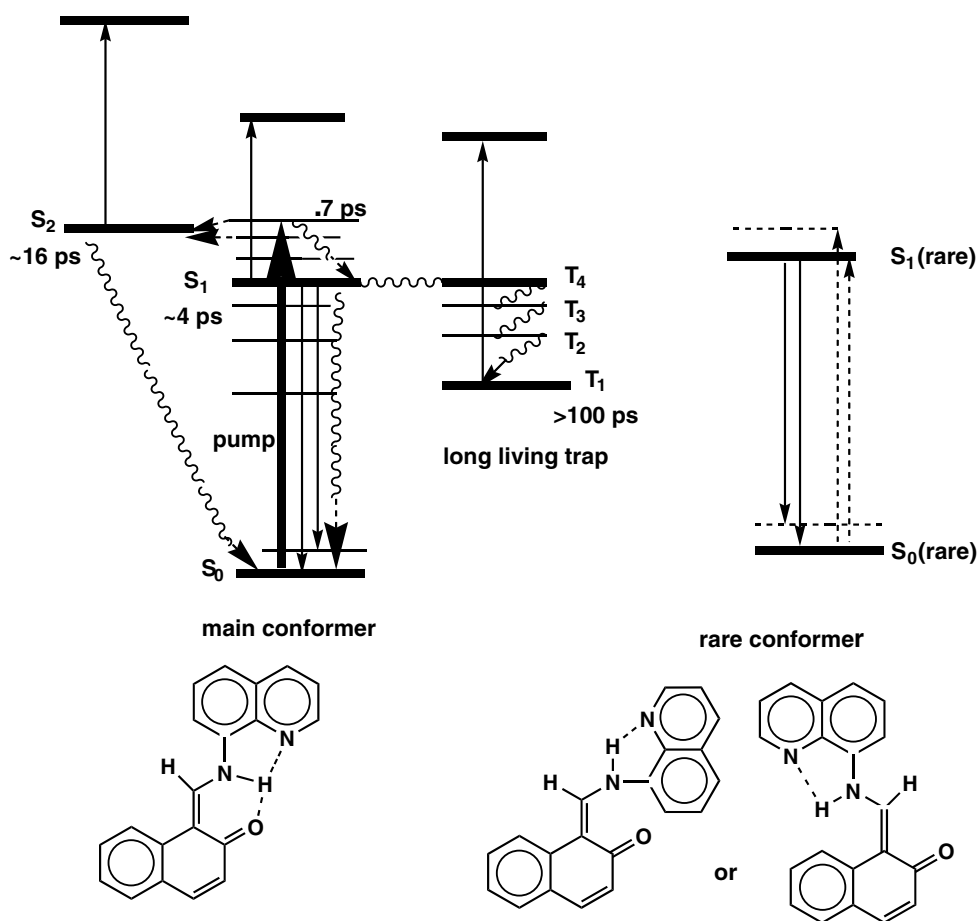


Fig. 4. Possible routes of relaxation of the excited HNAQ molecule with proposed structures of conformers contributing to the observed spectral and kinetic behavior. The orbital characters of the lowest electronic states are the following:  $S_1(\pi,\pi^*)$ ,  $S_2(n,\pi^*)$ ,  $T_4(n,\pi^*)$ ;  $T_1$ ,  $T_2$ ,  $T_3$  are triplet ( $\pi,\pi^*$ ) states. On the right side the possible rare conformers (with no hydrogen bond to the carbonyl group) are shown.

in the bleaching band, however one of its peaks, located at 457 nm, is hidden under the neighbouring absorption band.

## 5. Conclusions

We have used stationary spectroscopy techniques, ultrafast transient absorption measurements as well as TDDFT calculations to investigate the routes of relaxation of the excited HNAQ molecule. This compound is an exceptional Schiff base: its keto tautomer is not a product of the ESIPt reaction but is already present in the ground state. As such, it is not a photochromic structure in the classical sense of this word. The model presented here explains the most prominent features of the observed ultrafast events, which are: a very short lifetime of the stimulated emission, a finite risetime of the bleaching signal, a very fast risetime of the excited state emission bands and two different decay rates observed in the kinetics of transient signals. A closely related molecule, HNAN, plays a role of the model of the enol tautomer. A detailed comparative study of HNAN and HNAQ is in preparation.

## Acknowledgment

The valuable discussion with Jacek Waluk, Ph.D., is kindly acknowledged.

## References

- [1] E. Hadjoudis, in: H. Durr, H. Bouas-Laurent (Eds.), *Photochromism: Molecules and Systems*, Elsevier, Amsterdam, 1990, p. 685.
- [2] T. Elsaesser, H.J. Bakker (Eds.), *Ultrafast Hydrogen Bonding Dynamics and Proton Transfer Processes in Condensed Phase*, Kluwer Academic Publishers, Dordrecht, 2002.
- [3] *Photochromism: Memories and Switches*, Chem. Rev. 100 (2000) 5 (special issue).
- [4] F.M. Raymo, S. Giordani, Proc. Natl. Acad. Sci. USA 99 (2002) 4941.
- [5] Y. Huang, S. Wu, Y. Zhao, Opt. Express 12 (2004) 895.
- [6] *Spectroscopy and Dynamics of Elementary Proton Transfer in Polyatomic Systems*, Chem. Phys. 136 (2) (1989) (special issue).
- [7] Z. Rozwadowski, W. Schilf, B. Kamieński, Magn. Reson. Chem., in press.
- [8] T. Dziembowska, Z. Rozwadowski, A. Filarowski, P.E. Hansen, Magn. Reson. Chem. 39 (2001) S67.
- [9] M. Gavrančić, B. Kaitner, E. Mestrović, J. Chem. Crystallogr. 26 (1996) 23.
- [10] K.A. Abbas, S.R. Salman, S.M. Kanan, Z.A. Fataftah, Can. J. Appl. Spectrosc. 41 (1996) 119.
- [11] A. Ohshima, A. Momotake, T. Arai, J. Photochem. Photobiol. A 162 (2004) 473.
- [12] S.A. Kovalenko, A.L. Dobryakov, J. Ruthmann, N.P. Ernsting, Phys. Rev. A 59 (1999) 2369.
- [13] M.J. Frisch et al., GAUSSIAN 98 (Revision A.7), Gaussian Inc., Pittsburgh, PA, 1998.
- [14] E.K.U. Gross, W. Kohn, Adv. Quantum Chem. 21 (1990) 255.
- [15] S.J. Strickler, R.A. Berg, J. Chem. Phys. 37 (1962) 814.
- [16] W.H. Melhuish, Natl. Bur. Std. 378, Proc. Conf. NBS, Gaithersburg, 1972, p. 378.